Zeitschrift: IABSE proceedings = Mémoires AIPC = IVBH Abhandlungen
Band: 7 (1983)
Heft: P-66: Nonlinear temperature distribution and its effects on bridges

Artikel: Nonlinear temperature distribution and its effects on bridges
Autor: Elbadry, Mamdouh M. / Ghali, Amin
DOI: https://doi.org/10.5169/seals-37501

Nonlinear Temperature Distribution and its Effects on Bridges

Répartition non linéaire de la température et son effet sur les ponts

Nichtlineare Temperaturverteilung und ihre Auswirkung auf Brücken

M. M. ELBADRY
Graduate Student
The University of Calgary
Calgary, AB, Canada

A. GHALI
Professor of Civil Engineering
The University of Calgary
Calgary, AB, Canada

Mamdouh Elbadry, born 1953, received B.Sc. and M.Sc. degrees in Civil engineering from Cairo University in 1976 and the University of Calgary 1982.

Amin Ghali, born 1928, received his B.Sc. and M.Sc. degrees in civil engineering from Cairo University in 1950 and 1954 and Ph.D. degree from Leeds University, England 1957.

SUMMARY

This paper reviews the state of the art of the behaviour of bridge structures under nonlinear temperature distributions produced by weather conditions. Methods are discussed for prediction of distributions of temperature and the corresponding stresses in a bridge cross section. The effects of various climatological and geometrical parameters on the temperature and stress distributions in both concrete and composite bridges are discussed. The influence of cracking on the thermal response and the significance of thermal loading to ultimate capacity are discussed.

RÉSUMÉ

Cet article présente l'état actuel des connaissances sur le comportement des structures de ponts soumis à des répartitions de température non linéaires dues aux conditions climatiques. On discute des méthodes destinées à prévoir la répartition de la température et des contraintes correspondantes dans une section de pont. Les effets des différents paramètres climatologiques et géométriques sur les répartitions de température et de contraintes dans les ponts en béton et mixtes sont discutés. L'influence de la fissuration sur le comportement et l'effet des sollicitations d'origine thermique sur la résistance ultime sont brièvement discutés.

ZUSAMMENFASSUNG

In diesem Beitrag wird das Verhalten von Brückentragwerken untersucht, welche durch eine nichtlineare Temperaturverteilung infolge äusserer Wetterbedingungen beansprucht sind. Es werden Methoden zur Vorhersage der Temperatur- und Spannungsverteilung über den Brückenquerschnitt diskutiert. Die Auswirkungen der verschiedenen klimatischen und geometrischen Parameter werden auf die Temperatur- und Spannungsverteilungen in Stahlbeton- und Verbundträgern verfolgt. Schliesslich wird der Einfluss der Rissbildung auf das Tragverhalten und die Bedeutung dieser Zwangsbeanspruchung gegenüber der Traglast diskutiert.

1. INTRODUCTION

The design of bridge structures for temperature variations has traditionally been limited to the longitudinal movements induced by the maximum expected mean temperature changes. These movements are usually allowed to occur freely (or with minimum restraint) by provision of expansion joints. Recently, however, there has been a growing awareness that in spite of provision of joints, important thermal stresses occur, particularly in continuous bridges. Many observations have indicated that thermal loadings can seriously affect the serviceability and the structural integrity of such structures [15,21].

The sources of thermal loadings in bridges can be from the heat of hydration of cement in the early ages and from the effect of weather conditions over the life of the structure. The distribution of temperature throughout a bridge structure must be known if the resulting stresses, reactions and deformations are to be calculated. This paper discusses the sources of thermal loadings in bridges and reviews the methods of predicting the distribution of temperature through such structures. The significance of thermal stresses induced in both prestressed concrete and composite bridges is also discussed.

A concrete bridge structure under the effect of dead load may have cracks or may be free of cracking depending upon the design particularly on the amount of prestressing. These cracks affect considerably the stresses caused by temperature variation. This effect is briefly discussed here.

2. SOURCES OF HEAT IN A BRIDGE STRUCTURE

Variations of temperature in concrete bridges begin by the heat of hydration of fresh concrete. The temperature rise by the chemical process depends on the type and amount of cement, on the thickness of the concrete member, on the thermal insulation of the forms and on the temperature of the mixing water and surrounding air. A temperature rise of 30°C (54°F) to 50°C (90°F) can be expected in members thicker than about 0.50 m (1.6 ft) due to this source of heat [16].

Also, an exposed bridge deck is continuously losing and gaining heat -- from solar radiation, radiation to or from the sky or surrounding objects, and convection to or from the surrounding atmosphere. Temperature changes induced by these sources depend upon the geometry of the bridge cross section and on a number of other factors:

- Geographic location of the bridge (latitude and altitude).
- Orientation of the bridge axis with respect to the sun.
- Time of the day and season.
- Degree of cloudiness and turbidity of the atmosphere.
- Climatological conditions: expressed in terms of the diurnal variations of the ambient temperature and wind speed.
- Nature and colour of bridge deck surfaces: expressed in terms of solar radiation absorptivity, emissivity and surface convection coefficient.
- Thermal and physical properties of the constituent materials of the bridge: thermal conductivity, specific heat and density.

In the daytime and especially during the summer, the heat gain is greater than the heat loss, resulting in a temperature rise throughout the cross section. During a typical winter night, the converse is true, and the temperature in the superstructure drops. The heat flow processes for typical summer and winter conditions are shown in Fig. 1. Radiant energy from the sun is partially reflected and partially absorbed. Reflected energy does not influence bridge temperature; absorbed energy, however, heats the bridge deck surface and gives rise to a temperature gradient through the deck. The amount of radiation absorbed by a bridge deck is a function of the nature and colour of the surface. A dark,

rough surface has higher absorptivity than does a light, smooth surface and consequently absorbs more solar radiation. Some of the absorbed radiant energy is lost from the surface by convection and reradiation. Convective heat transfer from or to the atmosphere is a function of wind velocity, ambient air temperature, and deck surface temperature.

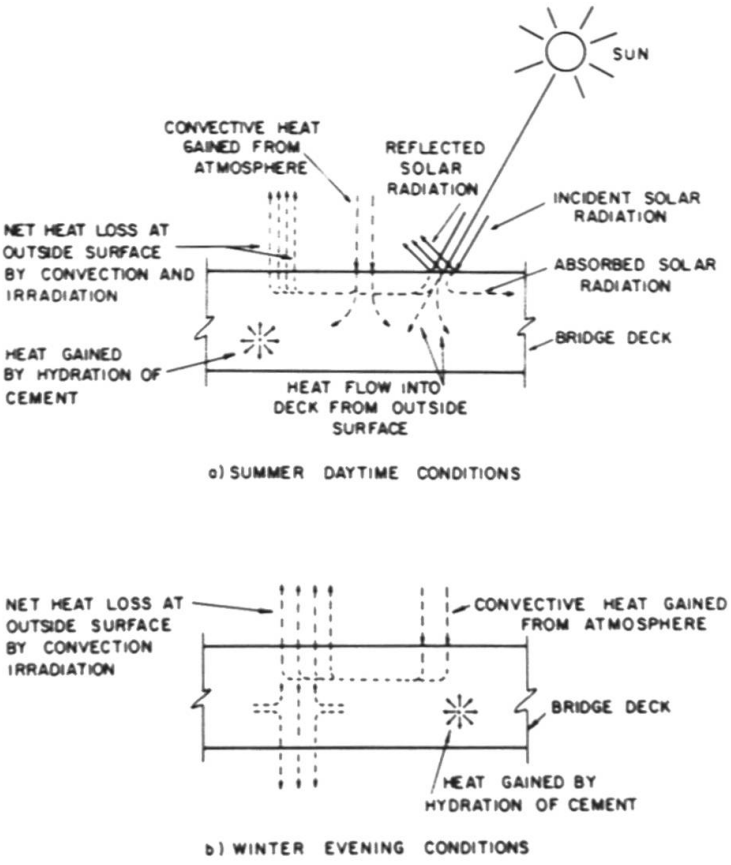

Fig. 1 Heat Gain and Loss Processes

3. BRIDGE TEMPERATURE

Because of the wide variations in climatic conditions in any given locality, a variety of temperature distributions is possible. In the literature, several such distributions have been observed or suggested based on theoretical studies. Included in these distributions are:

1. A linear temperature distribution in the deck slab and the top part of the web in a concrete box-section observed by Maher [18], (Fig. 2a).
2. Based on finite difference analyses, Priestley [22] suggested a combination of fifth degree parabolic and straight line variations over the webs and the top and bottom slabs of box and T girders (Fig. 2b).

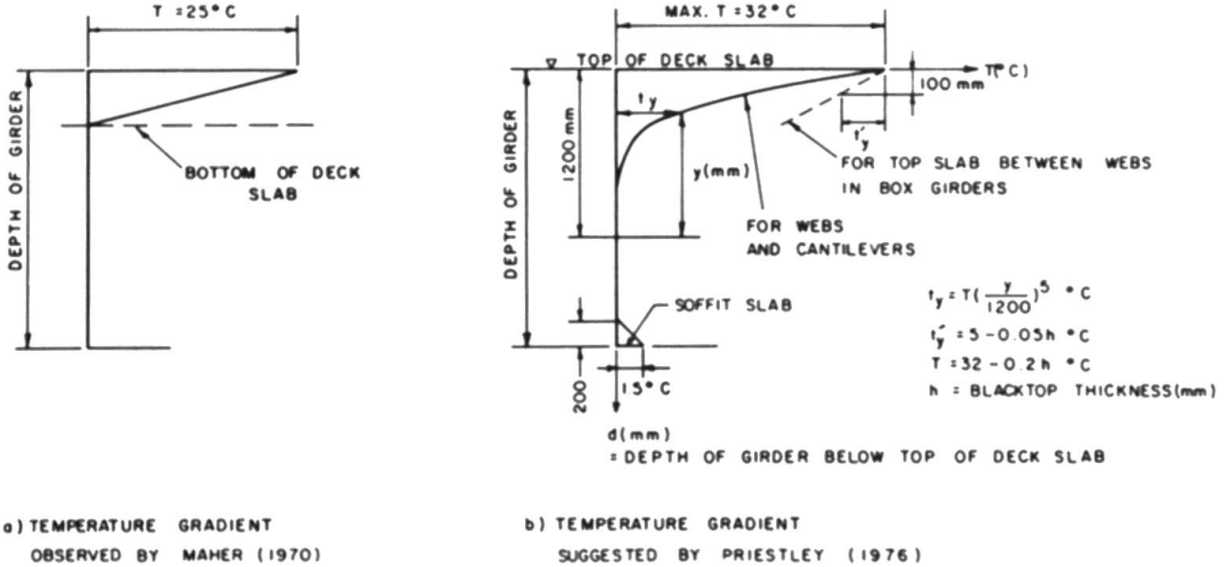

Fig. 2 Temperature Gradients in Box and T-Girders Observed or Suggested by Previous Investigators

When the bearings of a bridge allow horizontal translation, a rise of temperature that is uniform over the bridge cross section, does not produce stresses. Thus, for the purpose of stress calculations the temperature variation over the cross section may be measured from an arbitrary datum. The datum in Figs. 2a and b is taken as the temperature over the major part of the web, away from the top and bottom extremities.

It will be shown that the longitudinal stresses due to temperature heavily depend on the shape of the temperature distribution. Thus, the temperature distribution needs to be accurately predicted.

4. HEAT FLOW EQUATION

For the purpose of temperature and stress analyses, it may be assumed that the temperature is constant over the bridge length but varies from point to point within the cross-section and also with time. This assumption will be adopted all through this paper. The following well-known heat flow equation applies [3].

$$k_x \frac{\partial^2 T}{\partial x^2} + k_y \frac{\partial^2 T}{\partial y^2} + Q = \rho\, c \frac{\partial T}{\partial t} \tag{1}$$

where k_x and k_y are the anisotropic thermal conductivities in the x and y directions, respectively, of units W/m°C or Btu/(h ft °F); Q is the rate of heat per unit volume generated within the body (e.g. by hydration of cement), W/m^3 or $Btu/(h\ ft^3)$; ρ is the density, kg/m^3 or lb/ft^3; and c is the specific heat, J/(kg°C) or Btu/(lb°F). The quantity Q of heat generated by hydration of cement in concrete may be predicted by empirical equations (see Ref. [20]).

If the energy is transferred by the surrounding media to or from the boundary surface, the boundary conditions associated with Eq. 1 can be expressed by

$$k_x \frac{\partial T}{\partial x} n_x + k_y \frac{\partial T}{\partial y} n_y + q = 0 \tag{2}$$

where n_x and n_y are the direction cosines of the unit outward vector normal to the boundary surface and q is the boundary heat input or loss per unit area, W/m^2 or $Btu/(h\ ft^2)$.

The rate of energy transfer, q at the surfaces of a bridge structure is the sum of solar radiation, convection and irradiation

$$q = q_s + q_c + q_r \tag{3}$$

where $q_s(s,t)$ is the solar radiation, $q_c(s,t)$ is the convection and $q_r(s,t)$ is the irradiation from the surface to the surrounding air. Each of these quantities varies with the position s of the point considered on the surface and the time.

The heat transfer components of Eq. 3 are treated by the following simple expressions. The heat gain due to sun rays, i.e. short wave radiation, received by the structure can be expressed by

$$q_s = a\, I \tag{4}$$

where I(s,t) depends on the position s of the point on the surface of the structure, the inclination of this surface to the horizontal and the length of the

path of the sun ray through the atmosphere, which is in turn dependent upon the position on the earth and the time t of the day and the day of the year (see Refs. [5] and [6]). The dimensionless coefficient a is the fraction of I absorbed by the surface of the structure.

The heat lost or gained from the surrounding air by convection as a result of temperature differences between the bridge surface and the air is given by Newton's law of cooling as

$$q_c = h_c (T - T_a) \tag{5}$$

where h_c is the convection heat transfer coefficient, W/(m^2°C) or Btu/(h ft^2°F); T(s,t) is the temperature of the surface; and $T_a(t)$ is the air temperature at time t. In a box-girder bridge, $T_a(t)$ is different inside and outside the box. The convection heat transfer coefficient, h_c, is a function of many variables such as wind speed, surface roughness, and geometric configuration of the exposed structure. Its value is usually determined experimentally or calculated by empirical formulae [13,19].

The heat transfer between the bridge and the surrounding atmosphere due to long wave radiation, i.e. thermal irradiation, produces a nonlinear boundary condition which can be modeled by Stefan-Boltzman radiation law which may be conveniently rewritten in the form [13]:

$$q_r = h_r (T - T_a) \tag{6}$$

in which $h_r(s,t)$ is a radiation heat transfer coefficient defined as

$$h_r = C_s e [(T + T^*)^2 + (T_a + T^*)^2] (T + T_a + 2T^*) \tag{7}$$

where C_s is the Stefan-Boltzman constant = 5.677 x 10^{-8} W/(m^2°K^4) or 18.891 x 10^{-8} Btu/(h ft^2°R^4); e is the emissivity coefficient relating the radiation of the bridge structure (a gray body) to that of an ideal black body ($0 \leq e \leq 1$); and T* is a constant = 273.15 used to convert temperature in degrees Celsius, °C, to degrees Kelvin, °K, or = 459.67 to convert temperature in degrees Fahrenheit, °F, to degrees Rankin, °R.

The radiation heat transfer coefficient, h_r, cannot be calculated unless T(s,t) is known. However, it has been shown that h_r is only slightly temperature dependent [17] and thus in a time incremental solution, an approximate value can be calculated employing earlier values of T(s,t). Once the radiation coefficient is calculated, it can be treated similarly to the convection coefficient, h_c, and the effects of heat flow by convection and irradiation can thus be combined in an overall heat transfer coefficient

$$h = h_c + h_r \tag{8}$$

To find the temperature distribution over the thickness of a slab it is sufficient to seek a solution of one-dimensional simplified form of Eq. 1. The finite difference method can provide simple numerical solution and was adopted by several investigators [9,11,17,22]. The finite element method was also used for the same problem [23]. The two-dimensional heat flow Eq. 1 needs to be solved when the temperature variation is to be determined through the thickness and over the breadth of the slabs and webs of a box girder. The finite element method was efficiently used for this analysis [6,8,14,24].

The temperature distribution in the plates of steel box girders may be determined employing one dimensional model [4]. Because of the relatively small thickness of the steel plates (10 to 25 mm) and their high thermal conductivity, the temperature distribution may be assumed constant throughout the thickness but varies from point to point over the perimeter of the box and also with time.

5. MATERIAL PROPERTIES

The basic material properties that determine the thermal behaviour of bridge structures are: thermal conductivity, k; specific heat, c; thermal diffusivity, $k/\rho c$; and coefficient of thermal expansion, α. The literature reveals that these properties for a heterogeneous material such as concrete vary over a wide range and depend primarily upon the composition and moisture content. For example, for concrete of normal weight and within normal atmospheric temperature, the conductivity varies from 1.5 to 2.5 W/(m°C) or 0.87 to 1.45 Btu/(h ft°F) [2, 20]; specific heat ranges between 840 and 1170 J/(kg°C) or 0.20 and 0.28 Btu/(lb°F) [20]; the diffusivity varies from 0.7×10^{-6} to 1.4×10^{-6} m^2/s or 7.53×10^{-6} to 15.07×10^{-6} ft^2/s [2,12] and the coefficient of thermal expansion ranges from 7.2×10^{-6} to 10×10^{-6} $°C^{-1}$ or 4×10^{-6} to 5.56×10^{-6} $°F^{-1}$ [1].

6. CONSEQUENCES OF TEMPERATURE VARIATIONS

This section discusses the stresses caused by temperature in a bridge for which the bearings allow free horizontal translation. In a simply-supported span, uniform or linearly varying temperature over the depth of the cross section produces no stresses. With nonlinear temperature variation (Fig. 3b), the same bridge is subjected to stresses because of the restraint of temperature expansion that must occur by the different fibres. These stresses, which are self-equilibrating, are referred to as *eigenstresses* (Fig. 3c). In a continuous bridge, temperature change produces statically indeterminate reactions and internal forces whether the variation in temperature over the cross section is linear or nonlinear. The stresses due to these forces are referred to as *continuity stresses*. The eigenstresses and/or the continuity stresses can reach values above the tensile strength of concrete. Many cracks in prestressed concrete bridges are attributed to these effects which are usually neglected in design calculations. A temperature rise caused by the sun at the top surface of a continuous bridge produces positive moments which cause tensile stresses at the bottom fibres. A crack damage caused by this type of thermal stresses

otto

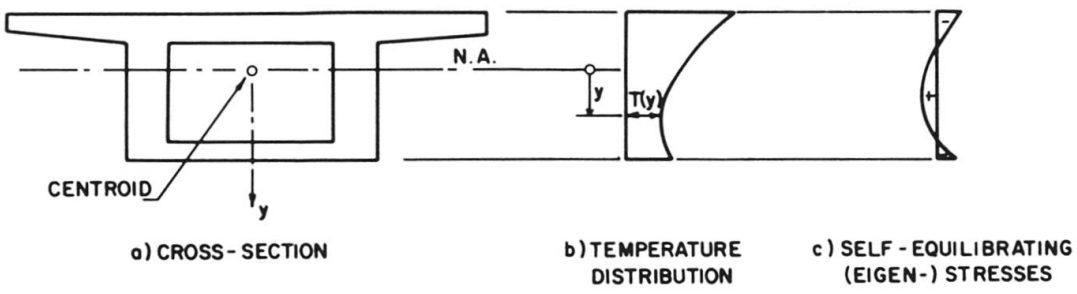

Fig. 3 Stresses in a Simply-Supported Beam

in two-span continuous beams in the vicinity of the intermediate supports was reported in Ref. [15].

Equally important temperature stresses occur in the transverse direction in a closed box section, which may be treated as a statically indeterminate plane frame.

7. STRESSES IN THE TRANSVERSE DIRECTION

Stresses in the transverse direction in a closed box may be calculated considering a plane frame made up of a strip between two cross sections of the box unit distance apart (Fig. 4a). The transverse stresses in the overhangs are zero and thus need not be considered in this analysis. Let the temperature rise in a section of this plane frame vary over the depth of the top slab as shown in Fig. 4b. For calculation of stresses, the displacement method of analysis [10] is convenient. The strain due to temperature is artificially restrained at all points; the restraining transverse stress at any fibre is

$$\sigma_{os} = -\frac{E\alpha}{1-\nu} T(y) \tag{9}$$

where E is Young's modulus of elasticity and ν is Poisson's ratio. At any section 1-1, the stress resultants are

$$N_{os} = \int_{\text{thickness}} \sigma_{os}\, dy \tag{10}$$

$$M_{os} = \int_{\text{thickness}} \sigma_{os}\, y\, dy \tag{11}$$

N_{os} and M_{os} vary with s as a result of variation of temperature or the thickness, and thus in the restrained condition tangential and transverse forces p_{os} and q_{os} must be applied (Fig. 4d). Considering the equilibrium of an element ds, Fig. 4c, the intensities of the restraining forces are:

$$p_{os} = -\frac{dN_{os}}{ds} \tag{12}$$

$$q_{os} = -\frac{d^2M_{os}}{ds^2} \tag{13}$$

The restraining forces for a typical member of the frame are shown in Fig. 4d. The artificial restraint is to be removed by the application of equal and opposite forces for all members and the corresponding stress $\bar{\sigma}_s$ is calculated from a conventional analysis. The actual stress due to temperature is

$$\sigma_s = \sigma_{os} + \bar{\sigma}_s \tag{14}$$

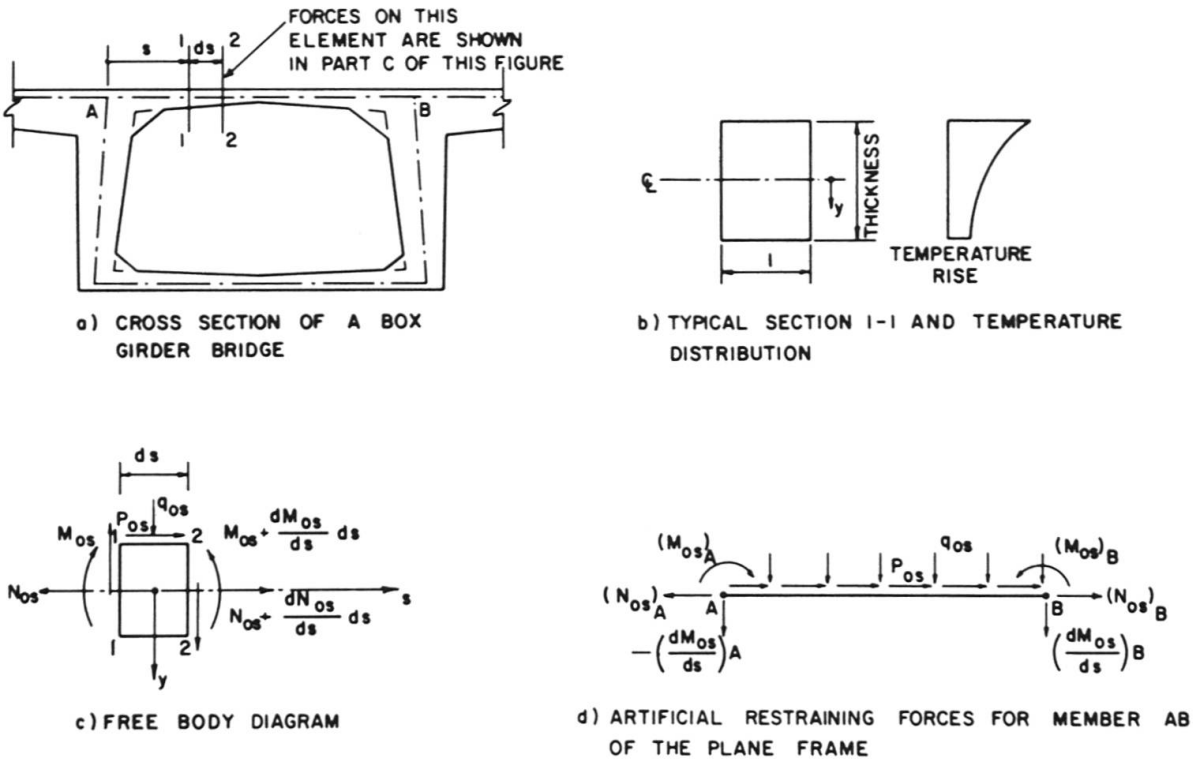

Fig. 4 Calculation of Stresses in Transverse Direction

8. EIGENSTRESSES

In the longitudinal direction the bridge is assumed to act as a beam, the procedure used for the transverse stresses can also be used for the longitudinal stress σ_ℓ. The procedure is applicable for a simply-supported or continuous bridge and the stresses thus obtained are the total of the eigen and continuity stresses. In this and the following section the stresses in a simply-supported and a continuous bridge of constant cross section are considered.

If the cross section and the temperature distribution are constant along the span of a simply-supported bridge, the strains due to temperature can be artificially restrained by applying forces only at the end cross sections. At a point (x,y) of any cross section the stress in the restraint state is (Fig. 5)

$$\sigma_{o\ell} = - \frac{E\alpha}{1-\nu} T(x,y) \tag{15}$$

The stress resultants at any section are (Fig. 5):

$$N_{o\ell} = \iint \sigma_{o\ell} \, dx \, dy \tag{16}$$

$$M_{ox\ell} = \iint \sigma_{o\ell} \, y \, dx \, dy \tag{17}$$

$$M_{oy\ell} = \iint \sigma_{o\ell} \, x \, dx \, dy \tag{18}$$

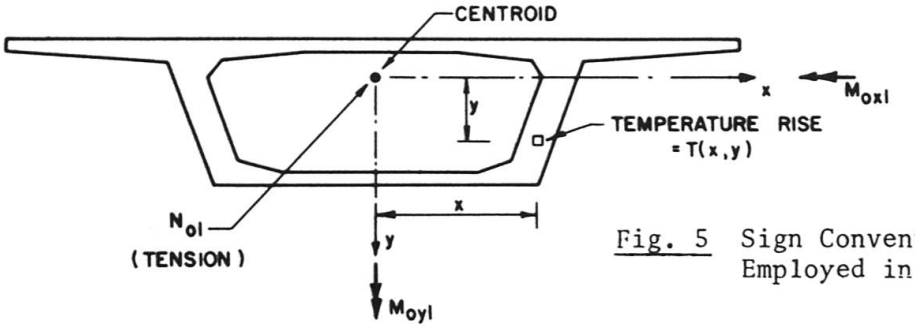

Fig. 5 Sign Convention for Symbols Employed in Eq. 19

Removal of the artificial restraints results in equal and opposite internal forces, which will produce stresses that are to be added to $\sigma_{o\ell}$ to obtain the eigenstresses,

$$\sigma_{\ell} = -\frac{E\alpha}{1-\nu} T - \left(\frac{N_{o\ell}}{A} + \frac{M_{ox\ell}}{I_x} y + \frac{M_{oy\ell}}{I_y} x\right) \tag{19}$$

where A, I_x and I_y are the area and the principal moments of inertia of the cross section.

The use of Eq. 19 and the significance of the eigenstresses are demonstrated by the following example of a statically determinate bridge. An example for the calculation of continuity stresses will be given in the following section.

Example 1: Find the stress distribution in a simply-supported concrete slab bridge assuming a temperature rise to vary over the depth as shown in Fig. 6b.

Equations 15 to 19 give

$$\sigma_{o\ell} = -\frac{E\alpha}{1-\nu} T \left(\frac{\bar{y}}{d}\right)^n \tag{20}$$

$$N_{o\ell} = -\frac{E\alpha T}{1-\nu} \frac{d}{1+n} \tag{21}$$

$$M_{ox\ell} = -\frac{E\alpha T}{1-\nu} \frac{nd^2}{2(n+1)(n+2)} \tag{22}$$

$$\sigma_{\ell} = \frac{E\alpha T}{1-\nu} \left[-\left(\frac{\bar{y}}{d}\right)^n - \frac{3n}{(n+1)(n+2)} \left(1 - \frac{2\bar{y}}{d}\right) + \frac{1}{n+1}\right] \tag{23}$$

The eigenstresses are zero at all fibres when the temperature distribution over the depth is linear (n=1).

Assuming the temperature rise to vary as a parabola of the third or fifth degree gives the values of the eigenstresses shown in Figs. 6d and e. The results of this example indicate how the eigenstresses depend upon the shape of the temperature distribution. For E = 30,000 MPa (4350 ksi), ν = 0.2, α = 10 x 10^{-6} °C^{-1} (5.56 x 10^{-6} °F^{-1}) and T = 40°C (72°F), the maximum compressive and tensile stresses in Fig. 6e are -7.14 and +2.4 MPa (-1.035 and +0.348 ksi).

The shape of the eigenstress distributions in I and box girders are of the same form as in Fig. 6d or e. The tensile stress in the central part of the height can produce cracks in the webs which are usually heavily stressed due to shear from gravity loads.

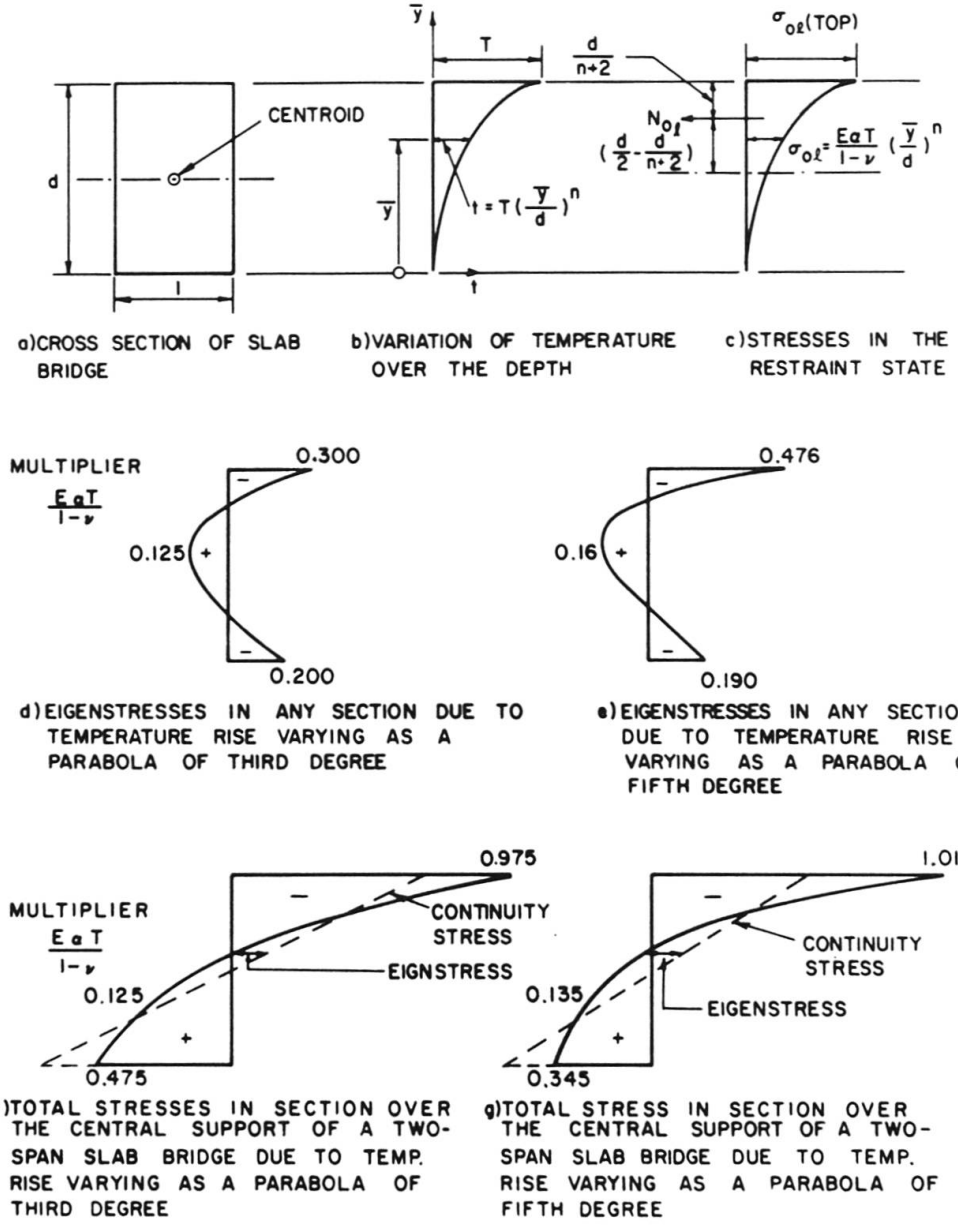

a)CROSS SECTION OF SLAB BRIDGE

b)VARIATION OF TEMPERATURE OVER THE DEPTH

c)STRESSES IN THE RESTRAINT STATE

d)EIGENSTRESSES IN ANY SECTION DUE TO TEMPERATURE RISE VARYING AS A PARABOLA OF THIRD DEGREE

e)EIGENSTRESSES IN ANY SECTION DUE TO TEMPERATURE RISE VARYING AS A PARABOLA OF FIFTH DEGREE

f)TOTAL STRESSES IN SECTION OVER THE CENTRAL SUPPORT OF A TWO-SPAN SLAB BRIDGE DUE TO TEMP. RISE VARYING AS A PARABOLA OF THIRD DEGREE

g)TOTAL STRESS IN SECTION OVER THE CENTRAL SUPPORT OF A TWO-SPAN SLAB BRIDGE DUE TO TEMP. RISE VARYING AS A PARABOLA OF FIFTH DEGREE

Fig. 6 Calculation of Total Stresses in a Slab Bridge Continuous Over Two Equal Spans (Examples 1 and 2)

In some circumstances when the temperature of the top surface of the slab drops suddenly as a result, say, of a deposited layer of hail during a summer day, tensile eigenstresses may be induced at the top and bottom fibres. These stresses when added to stresses from other loading conditions, may cause cracks at one or the other of the exterior surfaces of the slab.

9. CONTINUITY STRESSES

Consider a simply-supported bridge subjected to temperature change that varies over the cross section. The thermal curvature in the vertical plane in this statically determinate structure is

$$\psi = -\frac{M_{ox}}{EI_x} \tag{24}$$

Substitution of M_{ox} using Eqs. 15 and 17 gives

$$\psi = \frac{\alpha}{(1-\nu) I_x} \int T\, y\, dy \qquad (25)$$

If the same bridge is made continuous with other spans, the curvature ψ is restrained and statically indeterminate reactions and internal forces will develop producing continuity stresses which must be added to the eigenstresses. Figure 7 shows the reactions and continuity moments produced by a temperature rise in continuous beams of different number of spans. It can be seen that, for a given bridge, continuity stresses are proportional to the induced curvature ψ.

Example 2: Assuming that the bridge of Example 1 is continuous with another symmetrical span, find the temperature stresses at the central support.

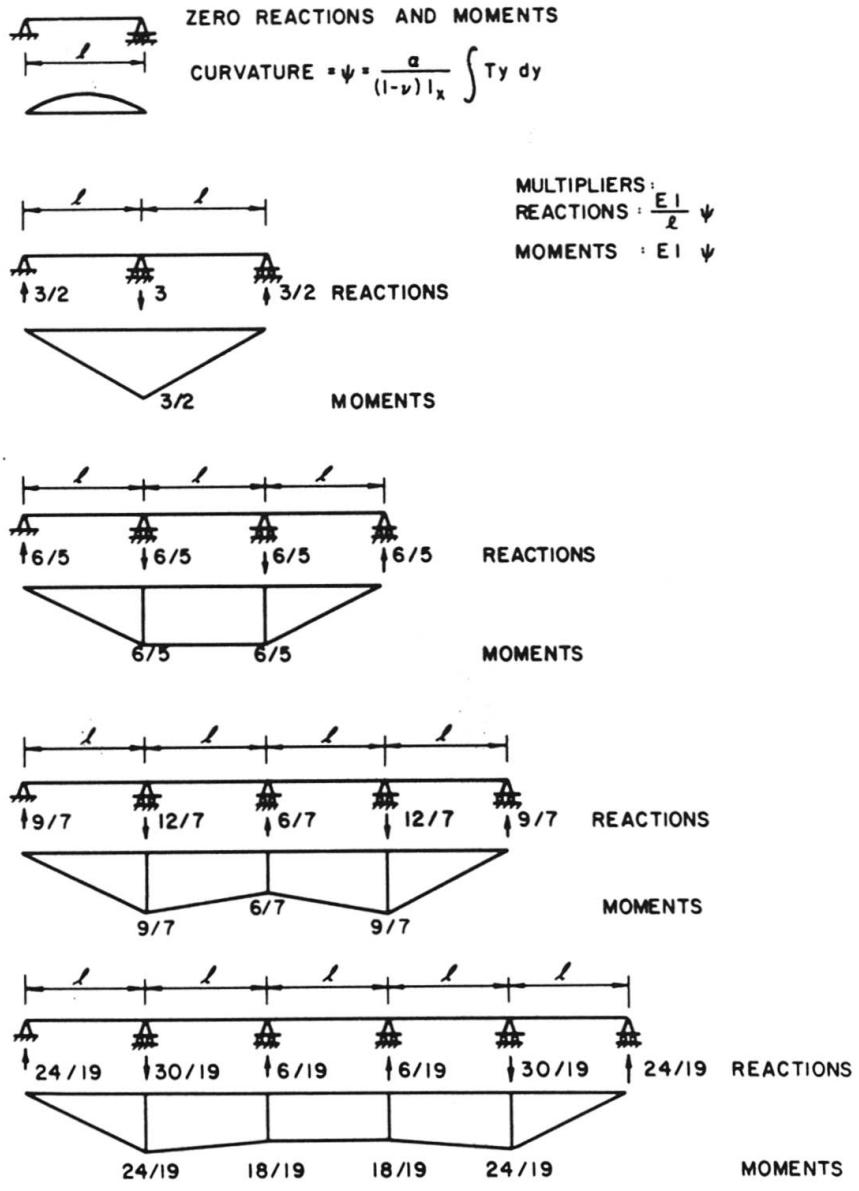

Fig. 7 Reactions and Bending Moments in Continuous Beams due to Temperature Rise (See Fig. 5)

The curvature in a simply-supported span (Eq. 25) is

$$\psi = \frac{2\alpha T}{d(1-\nu)} \left[\frac{3n}{(n+1)(n+2)}\right] \tag{26}$$

The continuity moment at the central support (see Fig. 7) is

$$M = \frac{3}{2} EI_x \psi = \frac{Ed^2 \alpha T}{4(1-\nu)} \left[\frac{3n}{(n+1)(n+2)}\right] \tag{27}$$

The total temperature stresses shown in Figs. 6f and g are the sum of the stresses due to M and the eigenstresses (Figs. 6d and e). For E = 30,000 MPa (4350 ksi), ν = 0.2, α = 10 x 10^{-6} °C^{-1} (5.56 x 10^{-6} °F^{-1}) and T = 40°C (72°F), the extreme fibre stresses in Fig. 6g are -15.18 and +5.175 MPa (-2.2 and +0.75 ksi).

10. EFFECTS OF VARIOUS PARAMETERS

Several parametric studies were conducted to investigate the effects of varying the orientation of the bridge axis, air temperature extremes, wind speed, surface conditions and shape and dimensions of the cross section on the temperature development and on the stresses induced in concrete and composite bridges. Only selected results of these studies will be presented here while details can be found in Refs. [4] and [6].

The bridges considered are assumed to be located in Calgary, Canada (51.03°N, altitude of 1050 m (3445 ft)). Climatological data, for different seasons, required for the analysis are given in Fig. 8. The dirunal variation of ambient air temperature is assumed to follow a sinusoidal cycle [4,8] between the minimum air temperature, min T_a, assumed to occur at 3:00 a.m., and the maximum value, max T_a, assumed to occur at 3:00 p.m. Thus

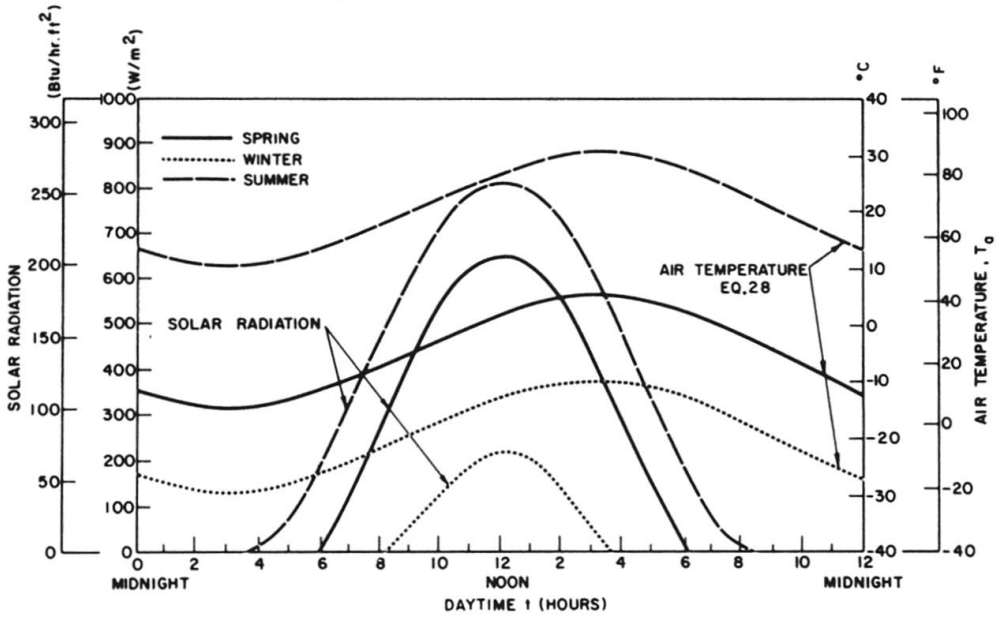

Fig. 8 Idealization of Diurnal Variation of Ambient Air Temperature and Solar Radiation Intensity Received on a Horizontal Surface for Different Seasons (Conditions at Calgary, Canada)

$$T_a(t) = A \sin \frac{\pi(t-9)}{12} + B \qquad (28)$$

where t is the hour of the day; A is the amplitude or one-half the daily range of air temperature; and B is the average daily temperature. The average temperature B may take any arbitrary value without affecting the stresses.

10.1 Effect of Season and Orientation of Bridge Axis

As indicated in Fig. 9a, the effect of bridge orientation on thermal curvature ψ induced in concrete bridges is not very pronounced during Spring or Summer, while in Winter, a change of 44% can occur in the maximum curvature when the bridge orientation is changed from North-South to East-West position. Thermal curvatures and eigenstresses are in general larger in Summer than they are in Spring or Winter. Temperature and eigenstress distributions along the centre line of one web corresponding to maximum curvatures in Summer are shown in Fig. 9b.

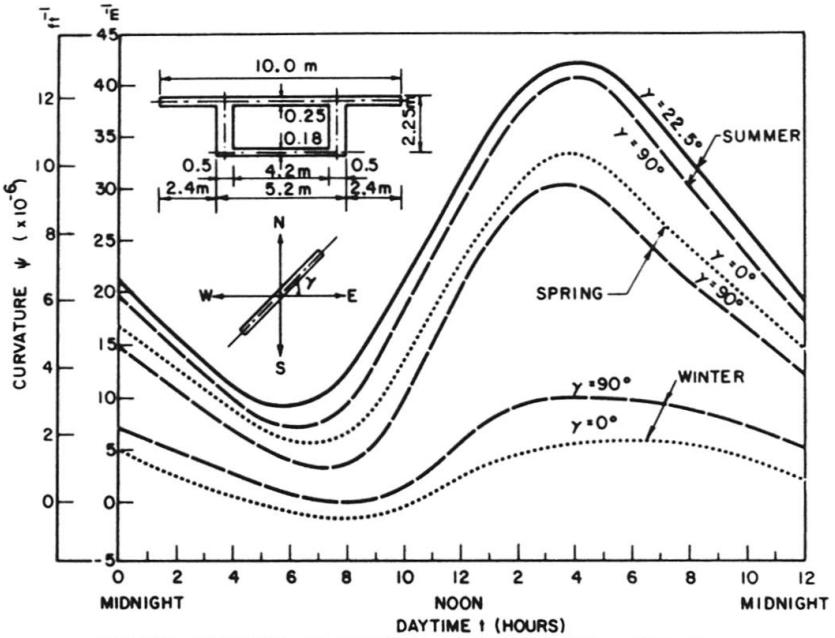

a) HOURLY VARIATION OF THERMAL CURVATURE FOR DIFFERENT ORIENTATIONS AND DIFFERENT SEASONS

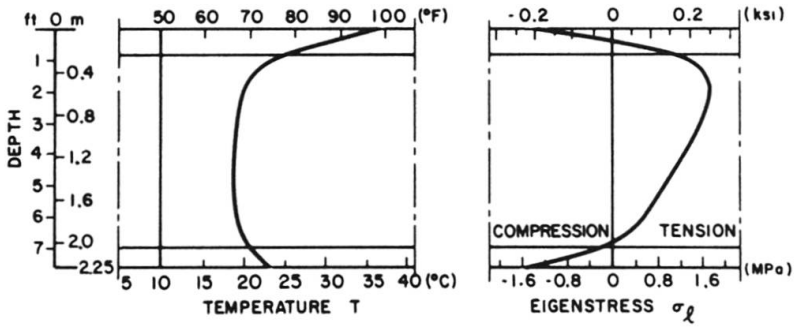

b) TEMPERATURE AND EIGENSTRESS DISTRIBUTIONS ALONG THE CENTRE LINE OF ONE WEB CORRESPONDING TO MAXIMUM CURVATURES FOR SUMMER CONDITIONS ($\gamma = 22.5°$)

Fig. 9 Effect of Season and Orientation of Bridge Axis on Thermal Curvature and Temperature and Eigenstress Distributions in Concrete Box Sections

For composite box girder bridges, it has been shown that the maximum temperature difference between steel and concrete develops in Winter in a bridge oriented East-West [4], while in Summer this orientation results in the smallest temperature difference. The temperature distribution with maximum temperature difference over the cross section of a composite bridge assumed to be located in Calgary, Canada, is shown in Fig. 10a. This distribution is for winter conditions and for East-West orientation of the bridge axis [4]. A difference of 45°C (81°F) between the maximum steel temperature and the average concrete temperature is expected. The corresponding distributions of eigen and total stresses at the central support of a bridge assumed continuous over two equal spans, 40 m (122 ft) each, are depicted in Fig. 10b. The compressive stresses in the steel reach approximately 90 MPa (13.0 ksi) while the maximum tensile stress developed in the concrete is about 2 MPa (0.29 ksi).

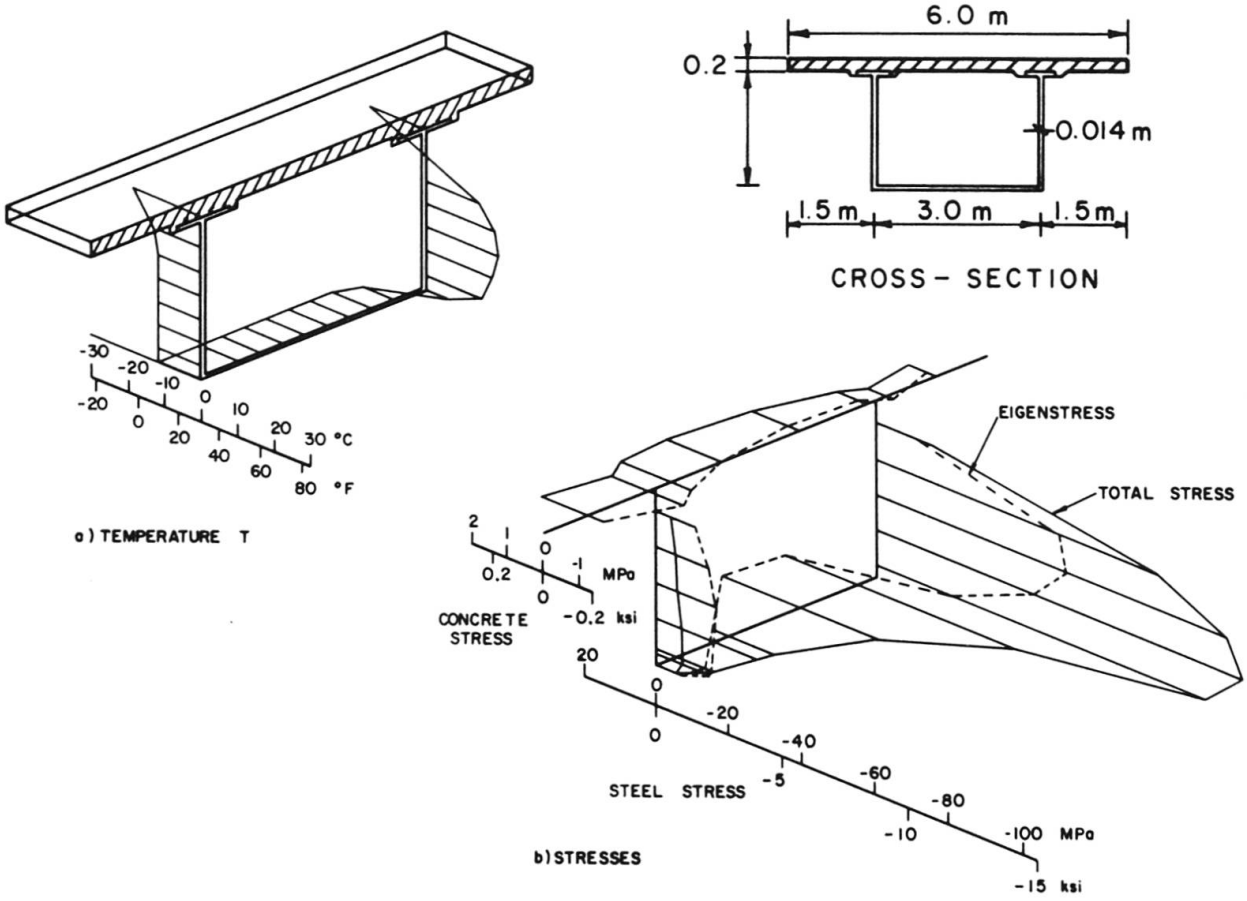

Fig. 10 Temperature and Eigen and Total Stress Distributions in a Section at the Central Support of a Two-Span Continuous Composite Box-Girder Bridge (Winter Conditions in Calgary, Canada, $\gamma = 0°$)

10.2 Effect of Daily Air Temperature Extremes

Figure 11 depicts the temperature, eigen and continuity stress distributions over one web of a concrete box girder continuous over two equal spans for which the range of air temperature variation, 2A, in a single day is assumed to be 20, 30 and 40°C (36, 54 and 72°F). The graphs of this figure represent the conditions at 4:00 p.m., the time of the day at which the continuity stresses are highest.

The figure indicates that higher values of A result in, as expected, higher stresses. The effect of change of A on the temperature of steel and concrete in a composite bridge are indicated in Fig. 12. For clarity, only the maximum temperature in steel is plotted in this figure when its value exceeds that of the ambient air.

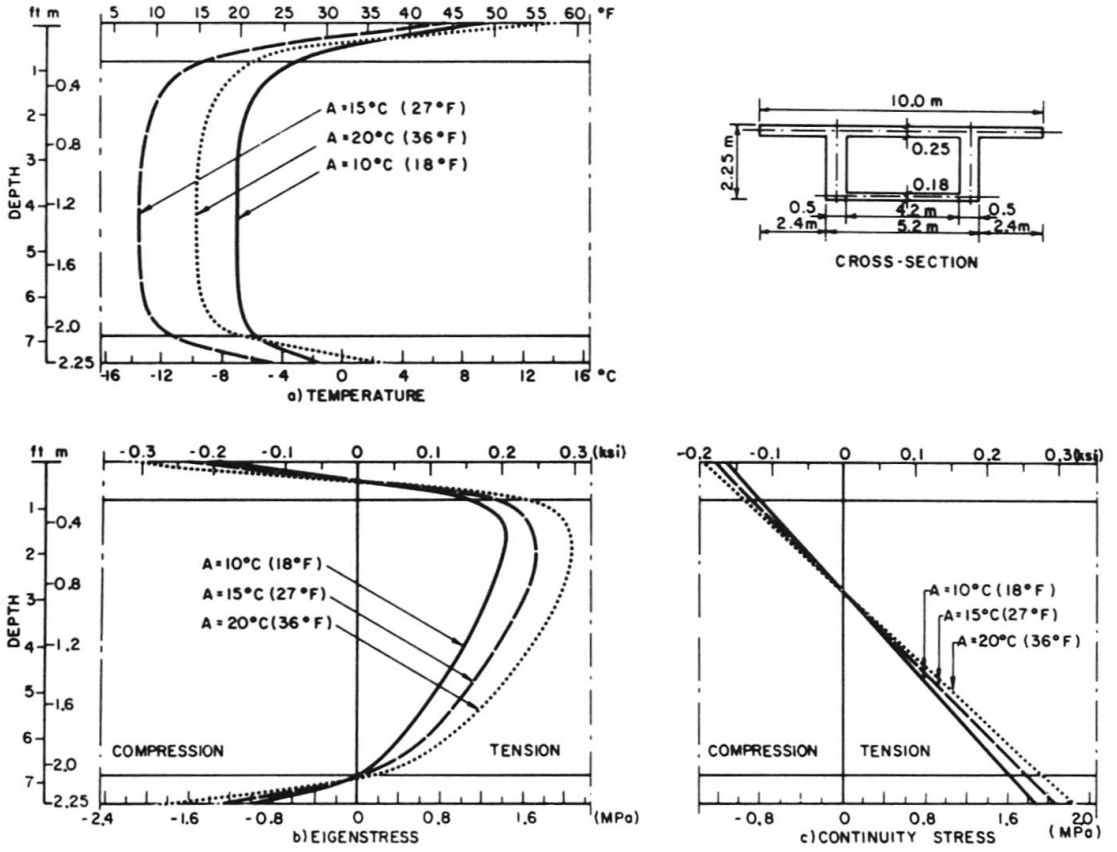

Fig. 11 Temperature and Stress Distributions Along One Web in a Section at the Central Support of a Two-Span Continuous Concrete Box-Girder Bridge Corresponding to Maximum Curvature (at 4:00 p.m.) for Different Ambient Temperature Extremes (Spring Conditions, $\gamma = 0°$)

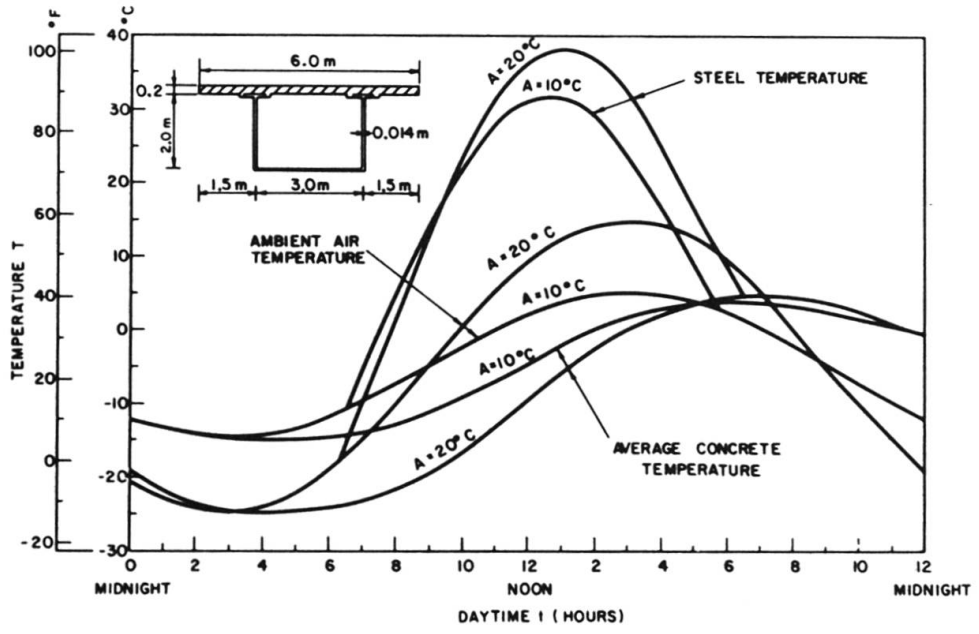

Fig. 12 Dirunal Variation of Maximum Temperature in Steel Box and Average Temperature in Concrete Deck for Different Ambient Temperature Extremes (Spring Conditions, $\gamma = 45°$)

10.3 Effect of Wind Speed

The wind speed influences the convection heat transfer between the external surfaces of the bridge and the surrounding air. As indicated in Fig. 13, higher wind speeds tend to bring the temperature of bridge surfaces closer to that of the ambient air. Higher wind speeds result in smaller curvatures and consequently reduced continuity stresses. The effect is smaller on the eigenstresses. It is thus obvious that bridges at exposed sites can be expected to have less thermal stress problems than sheltered bridges in urban environments.

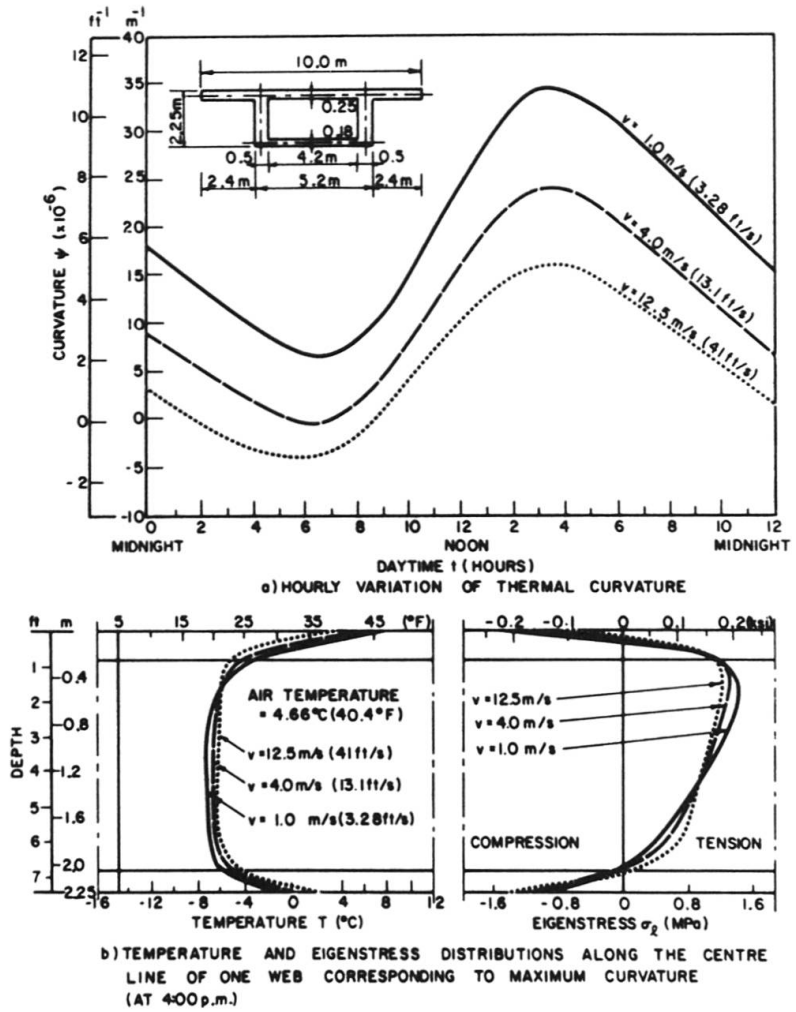

Fig. 13 Effect of Wind Speed on Thermal Curvature and Temperature and Eigenstress Distributions in Concrete Box Sections (Spring Conditions, $\gamma = 0°$)

10.4 Effect of Surface Conditions

Asphalt has higher absorptivity and emissivity coefficients (a = 0.9 and e = 0.92) compared to gray concrete surfaces (a = 0.5 and e = 0.88). The presence of a 50 mm (2 in) asphalt overlay on the concrete deck results in, as indicated in Fig. 14, an increase in the top surface temperature and in the thermal curvature and eigenstresses induced in concrete cross sections. On the contrary, a thin layer of fresh snow (a = 0.15 and e = 0.3) reduces each of these variables.

In a composite bridge, the surface condition of the steel box has a considerable effect on the temperature difference between steel and concrete. Figure 15 shows that a gray-black oxidized steel surface (a = 0.95) produces a temperature difference of 53°C (95°F) while a white surface (a = 0.15) reduces this difference to a mere 13.5°C (24°F).

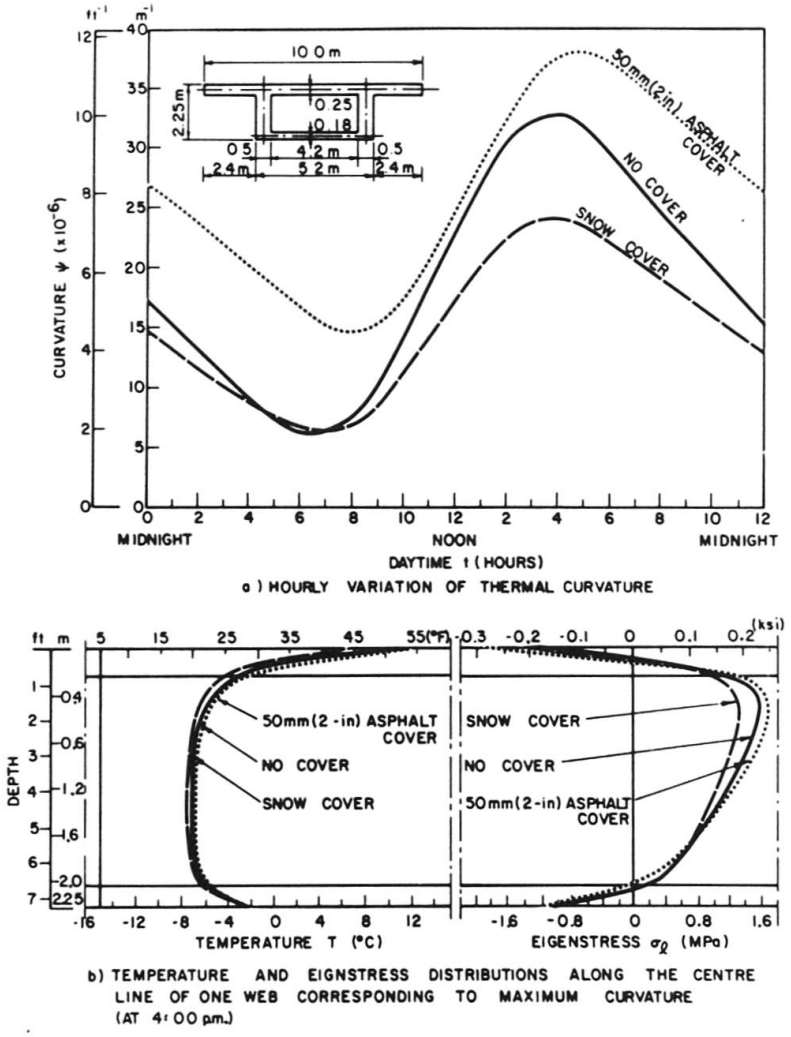

Fig. 14 Effect of Surface Cover on Thermal Curvature and Temperature and Eigenstress Distributions in Concrete Box Sections (Spring Conditions, $\gamma = 0°$)

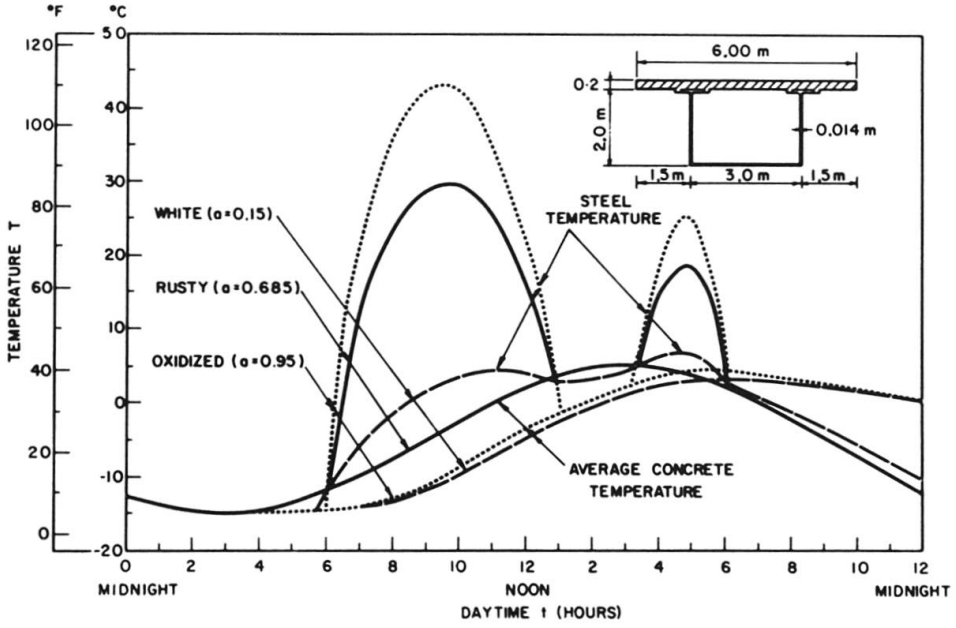

Fig. 15 Diurnal Variation of Maximum Temperature in Steel Box and Average Temperature in Concrete Deck for Different Absorptivities of the Steel Surface (Spring Conditions, $\gamma = 45°$)

10.5 Effect of Cross Section Shape and Depth

Figure 17 shows that concrete bridges of the same depth but with the cross section shapes shown in Fig. 16 have almost the same temperature distribution, eigenstresses and curvature. On the other hand, the temperature distribution varies considerably with the section depth. Figure 18 indicates that eigenstresses are higher when the depth is larger.

It can be shown that continuity stresses depend on the product of the depth and curvature (ψd). The relationship between the non-dimensional product ψd and the depth d is shown in Fig. 19 for the bridge sections in Fig. 16. The highest continuity stress is for the bridge with a depth 0.5 m (1.6 ft).

The increase in the depth of the composite bridges increases the area of the steel web exposed to the sun and hence the temperature difference between the steel and concrete. A decrease in the length of the overhangs has a similar effect on the temperature difference.

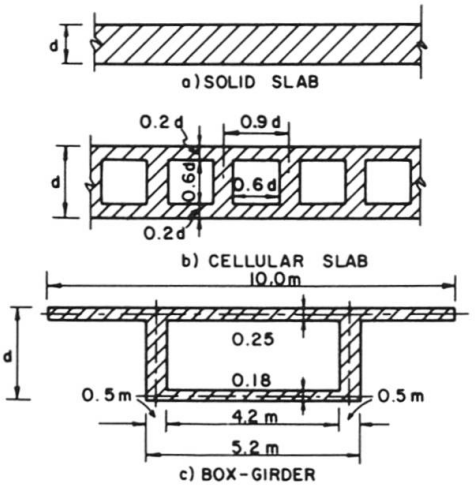

Fig. 16 Bridge Cross-Sections Analyzed to Study the Effects of Section Shape and Depth

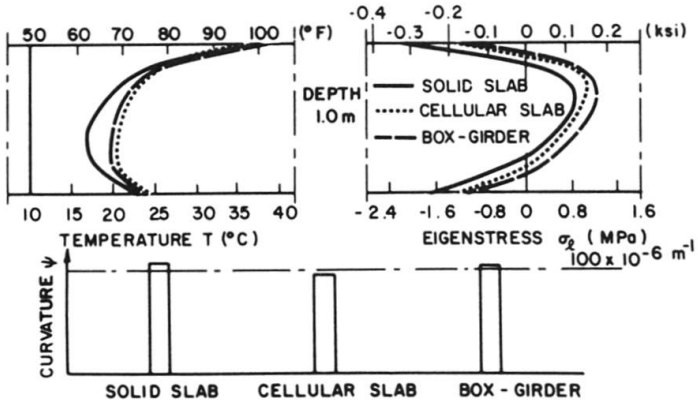

Fig. 17 Variation of Temperature, Eigenstresses and Curvatures in Cross Sections of Fig. 16 for the Same Depth (Summer Conditions, γ = 22.5°)

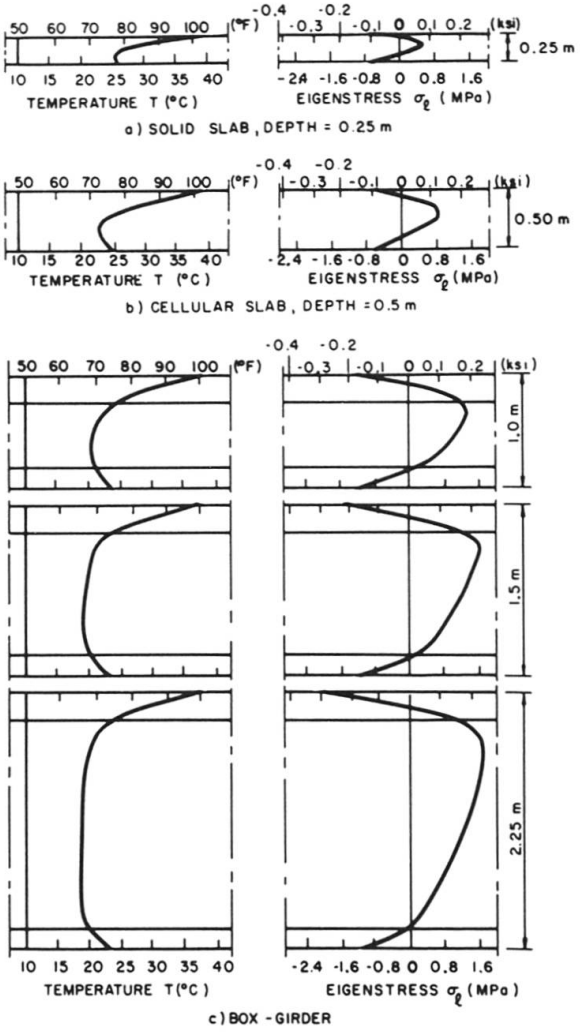

Fig. 18 Variation of Temperature and Eigenstresses in Cross Sections of Fig. 16 with Different Depths (Summer Conditions, γ = 22.5°)

Another major factor is the slope of the steel webs. Because of the smaller incidence angle of sun rays for sloped webs, the temperature differences decrease as the slope decreases.

The above results may be helpful in the development of code provisions or simplified rules for bridge design.

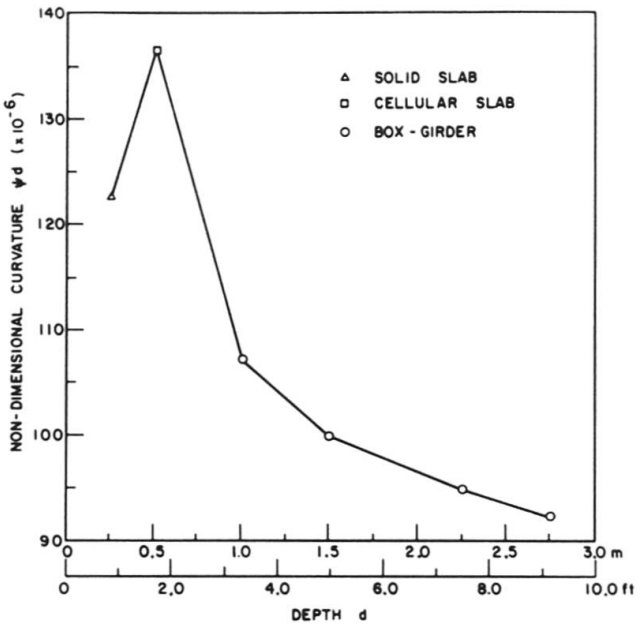

Fig. 19 Variation of Non-Dimensional Curvature with Cross-Sectional Depth for Concrete Sections of Figure 16 (Summer Conditions, $\gamma = 22.5°$)

11. EFFECT OF CRACKING ON THERMAL RESPONSE

High tensile stresses due to temperature cannot practically be avoided and cracking will have to occur. In a two-span continuous concrete box girder bridge, when the prestress force over the central support is relatively high resulting in small compressive stress at the bottom fibre at service load levels, temperature stresses may cause vertical cracks as shown in Fig. 20b. Partial prestressing and a sufficient amount of non-prestressed steel will help prevent or alleviate the consequence of this cracking. Cracks parallel to the bridge axis may occur in the bottom surface of the top slab due to thermal gradient through the thickness of the deck (Fig. 20c). Horizontal cracks may also occur in the web when significant horizontal thermal gradients exist through the web thickness (Fig. 20a).

Figure 21 illustrates the effect of cracking of concrete on the continuity moments and the significance of thermal loading at both service and ultimate load levels [22]. As can be seen, at ultimate load, the thermal moments are considerably reduced and are of less significance than at service loads, due to nonlinearity of the moment-curvature curve. Thus, it can be concluded that a feasible design would be to imply partial prestressing in combination with sufficient mild steel reinforcement and to rely on the reduction in flexural rigidity due to cracking to reduce thermal moments. The maximum values of thermal moments must, however, be considered for limit states of serviceability -- mainly for dimensioning the reinforcement to ensure that the cracks are finely distributed and crack width limitations are met.

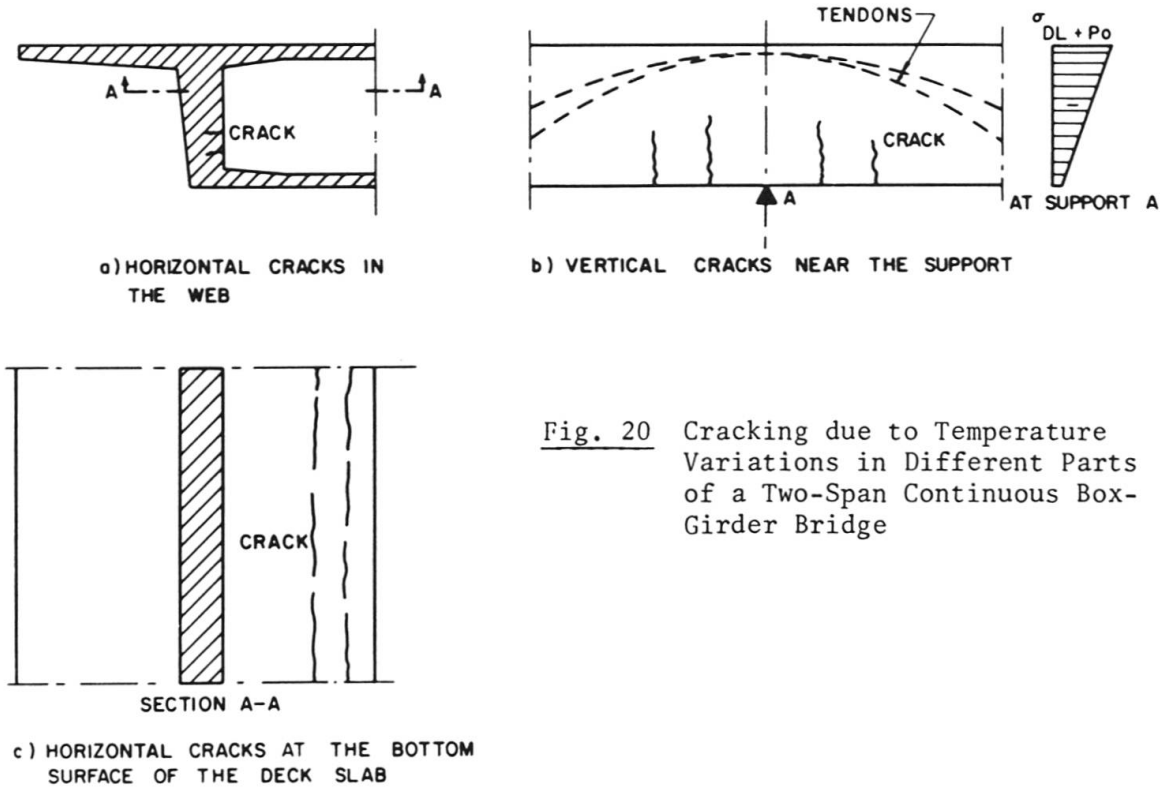

Fig. 20 Cracking due to Temperature Variations in Different Parts of a Two-Span Continuous Box-Girder Bridge

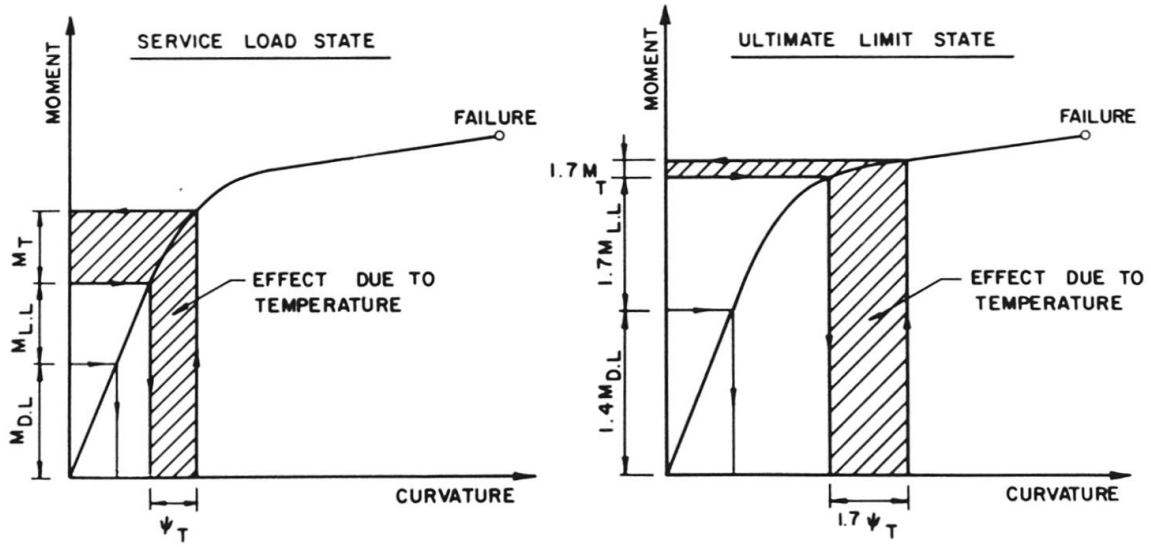

Fig. 21 Influence of Thermal Loading on Serviceability and Ultimate Capacity of Concrete Structures

12. SUMMARY AND CONCLUSION

The temperature distributions produced by the environment over the cross section of a bridge structure are generally non-planer and induce longitudinal as well as transverse stresses of substantial magnitude. The longitudinal stresses induced in a simply-supported bridge are referred to as eigenstresses while additional continuity stresses also develop due to temperature in a continuous, or statically indeterminate bridge. Analytical methods are available enabling prediction of temperature distribution over bridge cross section from data related to the situation of the bridge and weather conditions [7].

The largest eigen and continuity stresses can be induced in a concrete bridge of a given geometry during Summer when the solar radiation is maximum and the webs are protected by the shade of the overhangs. Also unfavorable conditions exist when the daily range of ambient temperature is large and the wind speed is minimum. An asphalt deck cover accentuates the stresses due to temperature. Increasing the overall cross-sectional depth increases the eigenstresses but decreases continuity stresses.

In composite steel-concrete box girders, the temperature difference between steel and concrete is the highest during Winter in an East-West oriented bridge. Extreme diurnal variation of the ambient temperature and minimum wind speed are unfavorable. Conditions of dark surface of the steel box, snow cover on the concrete deck, small or no overhanging cantilever and deep steel box also increase the temperature difference.

Temperature variations may cause cracking of concrete in different parts of box girder bridges. This cracking produces stress redistribution and substantial relief of temperature stresses. The use of partial prestressing to reduce thermal stress levels and control thermal cracking would seem reasonable.

Thermal effects are generally insignificant when assessing the ultimate load characteristics of a concrete bridge, and need only be considered for serviceability checks.

NOTATION

The following symbols are used in this paper:

A	=	one-half of the daily air temperature range
a	=	solar radiation absorptivity coefficient
B	=	daily average of air temperature
C_s	=	Stefan-Boltzman constant, 5.677×10^{-8} W/(m^2 °K^4) or 18.891×10^{-8} Btu/(h ft^2 °R^4)
c	=	specific heat, J/(kg °C) or Btu/(lb °F)
d	=	total cross sectional depth
E	=	modulus of elasticity
e	=	emissivity coefficient
$h(s,t)$	=	overall heat transfer coefficient at surface s at time t, W/(m^2 °C) or Btu/(h ft^2 °F)
h_c	=	convection heat transfer coefficient, W/(m^2 °C) or Btu/(h ft^2 °F)
$h_r(s,t)$	=	radiation heat transfer coefficient, W/(m^2 °C) or Btu/(h ft^2 °F)
$I(s,t)$	=	solar radiation intensity on surface s at time t, W/m^2 or Btu/(h ft^2)
I_x and I_y	=	moments of inertia of a cross section about its centroidal x and y-axes
k_x and k_y	=	anisotropic thermal conductivities in the x and y directions, W/(m °C) or Btu/(h ft °F)
M_{os}	=	restraining bending moment in the transverse direction (artificial)
$M_{ox\ell}$ and $M_{oy\ell}$	=	restraining end moments in the longitudinal direction (artificial)
N_{os} and $N_{o\ell}$	=	restraining end forces in the transverse and longitudinal directions, respectively, (artificial)
n_x and n_y	=	direction cosines of the unit outward normal to the boundary surface
p_{os}	=	tangential distributed restraining forces in the transverse direction (Fig. 4d)
Q	=	rate of heat generation, W/m^3 or Btu/(h ft^3)

q_c, q_r and q_s = heat flow due to convection, thermal irradiation and solar radiation, respectively, W/m^2 or $Btu/(h\ ft^2)$
q_{os} = lateral distributed restraining forces in the transverse direction (Fig. 4d)
T = temperature
T^* = conversion temperature (Eq. 7)
T_a = air temperature
t = time or hour of the day
α = coefficient of thermal expansion, $°C^{-1}$ or $°F^{-1}$
ν = Poisson's ratio
ρ = density of the material, kg/m^3, or lb/ft^3
σ_{os} and $\sigma_{o\ell}$ = stresses in the transverse and longitudinal directions, respectively, due to temperature when the strains are artificially restrained
$\bar{\sigma}_s$ = stresses in the transverse direction corresponding to removal of artificial restraint
σ_ℓ = eigenstress
ψ = curvature in the vertical direction in a simply-supported bridge, m^{-1} or ft^{-1}

REFERENCES

1. BERWANGER, C. and SARKAR, P.A., Effects of Temperature and Age on the Thermal Expansion and Modulus of Elasticity of Concrete, Behaviour of Concrete Under Temperature Extremes, ACI Special Publication SP-39, Detroit, 1973, pp. 1-22.

2. BRUY, E., Uber den Abbau Instationärer Temperaturspannungen in Betonkörpern durch Rissbildung, Doctoral Dissertation, Universität Stuttgart, Stuttgart, January 1973.

3. CARSLAW, H.S. and JAEGER, J.C., Conduction of Heat in Solids, 2nd ed., Clarendon Press, Oxford, England, 1959.

4. DILGER, W.H., GHALI, A., CHAN, M., CHEUNG, M.S. and MAES, M., Temperature Stresses in Composite Box-Girder Bridges, Proceedings American Society of Civil Engineers, Journal of the Structural Division, Vol. 109, No. ST6, Proceedings Paper 18064, June 1983, pp. 1460-1478.

5. DUFFIE, J.A. and BECKMAN, W.A., Solar Energy Thermal Processes, John Wiley and Sons, Inc., 1974.

6. ELBADRY, M.M. and GHALI, A., Temperature Variations in Concrete Bridges, Proceedings American Society of Civil Engineers, Journal of the Structural Division, (in print)

7. ELBADRY, M.M. and GHALI, A., Users' Manual for Computer Program FETAB: Finite Element Thermal Analysis of Bridges, Research Report No. CE82-10, Department of Civil Engineering, The University of Calgary, Canada, October 1982.

8. EMANUEL, J.H. and HULSEY, J.L., Temperature Distributions in Composite Bridges, Journal of the Structural Division, ASCE, Vol. 104, No. ST1, Proceedings Paper 13474, January 1978, pp. 65-78.

9. EMERSON, M., The Calculation of the Distribution of Temperature in Bridges, Transport and Road Research Laboratory, TRRL Report LR 561, Crowthorne, Berkshire, England, 1973.

10. GHALI, A. and NEVILLE, A.M., Structural Analysis - A Unified Classical and Matrix Approach, 2nd ed., Chapman and Hall, London, England, 1978.

11. HUNT, B. and COOKE, N., Thermal Calculations for Bridge Design, Journal of the Structural Division, ASCE, Vol. 101, No. ST9, Proc. Paper 11545, September 1975, pp. 1763-1781.

12. KEHLBECK, F., Einfluss der Sonnenstrahlung bei Brückenbauwerken, Werner-Verlag, Düsseldorf, Germany, 1975.

13. KREITH, F., Principles of Heat Transfer, 3rd ed., Intext Educational Publishers, New York, N.Y., 1973.

14. LANIGAN, A.G., The Temperature Response of Concrete Box Girder Bridges, School of Engineering Report No. 94, Thesis presented to the University of Auckland, Auckland, New Zealand, 1973, in partial fulfillment of the requirements for the degree of Doctor of Philosophy.

15. LEONHARDT, F. and LIPPOTH, W., Folgerungen aus Schäden an Spannbetonbrücken, Beton-und Stahlbetonbau, Vol. 65, Heft No. 10, October 1970, pp. 231-244.

16. LEONHARDT, F., Prevention of Damages in Bridges, Proceedings of the Ninth International Congress of the FIP, Stockholm, Commission Reports, Vol. 1, June, 1982.

17. MAES, M.A., Effects of Environmental Material Characteristics on the Behaviour of Concrete Structures, Thesis presented to the University of Calgary, Calgary, Alberta, Canada, 1980, in partial fulfillment of the requirements for the degree of Master of Science in Engineering.

18. MAHER, D.R.H., The Effects of Differential Temperature on Continuous Prestressed Concrete Bridges, Civil Engineering Transactions, Institution of Engineers, Australia, Vol. CE12, No. 1, Paper 273, April 1970, pp. 29-32.

19. McADAMS, W.H., Heat Transmission, 3rd ed., McGraw-Hill Book Co., Inc., New York, N.Y., 1954.

20. NEVILLE, A.M., Properties of Concrete, 2nd ed., Pitman Publishing, London, 1973.

21. PRIESTLEY, M.J.N., Effects of Transverse Temperature Gradients on Bridges, Central Laboratories, New Zealand Ministry of Works, Report No. 394, October, 1971.

22. PRIESTLEY, M.J.N., Design of Concrete Bridges for Temperature Gradients, ACI Journal, May 1978, pp. 209-217.

23. RAHMAN, F. and GEORGE, K.P., Thermal Stresses in Skew Bridge by Model Test, Journal of the Structural Division, ASCE, Vol. 106, No. ST1, Proc. Paper 15112, January 1980, pp. 39-59.

24. SYMKO, Y.B., Transient Heat Conduction and Thermoelastic Analysis of Three-Span Composite Highway Bridge, Thesis presented to the University of Ottawa, Ottawa, Canada, 1979, in partial fulfillment of the requirements for the degree of Doctor of Philosophy.